(2)

OFFICE OF NAVAL RESEARCH

Grant # N0001489J1848

R&T Code 413u002

Technical Report No. 12

Diamond Nucleation on Surfaces Using Carbon Clusters

by

R.J. Meilunas, R.P.H. Chang

prepared for publication in the

Journal of Materials Research

Northwestern University
Dept. of Materials Science and Engineering,
Evanston, IL 60208

May 1993

REPORT DOCUMENTATION PAGE

Form Approved
OMB No. 0704-0188

1. AGENCY USE ONLY (Leave blank)	2. REPORT DATE	3. REPORT TYPE AND DATES COVERED
	May 1993	Technical

4. TITLE AND SUBTITLE

Diamond Nucleation on Surfaces Using Carbon Clusters

5. FUNDING NUMBERS

G N0001489J1848
R&T code 413u002

6. AUTHOR(S)

R.J. Meilunas, R.P.H. Chang

7. PERFORMING ORGANIZATION NAME(S) AND ADDRESS(ES)

Materials Science & Engineering Dept.
Northwestern University
2225 Sheridan Road
Evanston, IL 60208

8. PERFORMING ORGANIZATION REPORT NUMBER

Technical Report #12

9. SPONSORING/MONITORING AGENCY NAME(S) AND ADDRESS(ES)

Chemistry Division
Office of Naval Research
800 N. Quincy Street
Arlington, VA 22217-5000

10. SPONSORING/MONITORING AGENCY REPORT NUMBER

11. SUPPLEMENTARY NOTES

12a. DISTRIBUTION/AVAILABILITY STATEMENT

This document has been approved for public release and sale; its distribution is unlimited.

12b. DISTRIBUTION CODE

13. ABSTRACT *(Maximum 200 words)*

Thin solid films of C_{60} and C_{70} have been used as nucleation layers for the growth of diamond thin films on a variety of substrate surfaces, including metal, insulator and semiconductors. Compared to other forms of carbon, such as graphite, amorphous carbon, soot, etc. it is found that the nucleation density on C_{70} is equivalent to that of diamond seeds themselves. On the other hand, diamond nucleation of C_{60} is less favorable. We argue from our experiments that the reason for C_{70} to have such favorable nucleating properties is its chemical stability and geometry. A working model is proposed to explain the nucleation of diamond on solid C_{70} films. Application of this work extending to the growth of diamond on a wide range of substrates is also discussed.

14. SUBJECT TERMS	15. NUMBER OF PAGES
Diamond Nucleation; carbon clusters	58
	16. PRICE CODE

17. SECURITY CLASSIFICATION OF REPORT	18. SECURITY CLASSIFICATION OF THIS PAGE	19. SECURITY CLASSIFICATION OF ABSTRACT	20. LIMITATION OF ABSTRACT
Unclassified	Unclassified	Unclassified	UL

Diamond Nucleation on Surfaces Using Carbon Clusters

R.J. Meilunas* and R.P.H. Chang
Dept. of Materials Science and Engineering
Northwestern University, Evanston, IL 60208

ABSTRACT

Thin solid films of C_{60} and C_{70} have been used as nucleation layers for the growth of diamond thin films on a variety of substrate surfaces, including metal, insulator and semiconductors. Compared to other forms of carbon, such as graphite, amorphous carbon, soot, etc. it is found that the nucleation density on C_{70} is equivalent to that of diamond seeds themselves. On the other hand, diamond nucleation of C_{60} is less favorable. We argue from our experiments that the reason for C_{70} to have such favorable nucleating properties is its chemical stability and geometry. A working model is proposed to explain the nucleation of diamond on solid C_{70} films. Application of this work extending to the growth of diamond on a wide range of substrates is also discussed.

I. Introduction

The success in growing thin diamond films using chemical vapor deposition methods has stimulated interest in the unique properties of diamond for potentially new technological applications. As an example, diamond has the combined properties of good electrical insulation, high thermal conductivity and low dielectric constant which make it well suited for use in device packaging and multi-chip module technologies. The extreme hardness and wide optical bandgap of diamond would also provide an excellent protective coating material for a variety of optical applications. The chemical inertness and hardness of diamond thin films would also find wide utilization as a protective coating against corrosion and wear in the cutting tool and metal working industries.

A number of different deposition techniques have been developed to deposit diamond thin films.[1,2,3,4,5] A fundamental problem encountered in most deposition methods is the limited understanding and controllability of diamond nucleation on non-diamond substrates. At present, the most common method to obtain substantial nucleation of diamond on non-diamond substrates is a pretreatment step. This pretreatment procedure is regularly accomplished by simply polishing the sample with diamond grit or paste before placing it in the deposition chamber. Without some type of diamond seeding, not enough diamond crystallites nucleate

on the surface of most materials in a reasonable amount of time to eventually grow and coalesce into continuous films. Such pretreatments are also not easily adapted towards coating large or non-planar surface areas.

In this paper we provide a more comprehensive discussion on the nucleation method described in an earlier publication [6] . This technique eliminates the need for surface abrasion and diamond seeding by usirg thin layers of fullerene films sublimated onto various non-diamond substrates. The thin fullerene layer produces a large number of nucleation sites suitable for the formation of continuous diamond films. The specificity of the type of fullerene is found to aid in elucidating the mechanism for diamond nucleation in low pressure CVD.

II. Background

Detailed experimental studies of the effects of substrate abrasion and seeding with diamond grit have been reported.[7] Recently, using high resolution transmission electron microscopy, Iijima et al [8] have demonstrated the effects of polishing the Si substrates on diamond nucleation. They observed that even after extensive cleaning of the diamond grit polished Si substrates, small "diamond dust " particles of nanometer size remain on the Si surface. The dust particles act as seeds for diamond nucleation on the substrate. This represents more of a form of homoepitaxy on isolated, randomly oriented, single crystal diamond than any type

of heteroepitaxy.

Earlier reports of enhancing diamond nucleation on unpolished, non-diamond substrates by various methods have been limited and inconclusive about nucleation mechanisms. These include enhancement with the use of diamond - like carbon films [9] , dc biasing [10] , fluorinated plasmas [11] , thin metal overlayers [12] , perylene derivatives [13] and even fingerprints [14] . However, with the exception of dc biasing, none of the above methods has produced as significant a degree of nucleation enhancement as that obtained by the simple method of polishing with diamond grit.

Various theoretical studies have proposed possible diamond forming precursors on which to nucleate diamond. Matsumoto and Matsui [15] were the first to identify several hydrocarbon cage compounds as possible diamond cluster embryos or "seeds" which included adamantane, tetracyclododecane, hexacyclopentadecane and dodecahedrane. The adamantane molecule, $C_{10}H_{16}$, represents the smallest combination of carbon atoms which possess the diamond unit structure (three six membered rings in a chair coordination). The other compounds represent twinned diamond embryos and were proposed as the precursors to the five fold twinned diamond microcrystals which are found prevalent in CVD diamond thin films.

From simple atomic structure comparisons, one can easily generate the diamond lattice from the above hydrocarbon cage compounds by simple hydrogen abstraction followed by carbon addition. Nevertheless, thermodynamic considerations show these molecules to be quite unstable in the harsh environment used

to grow diamond films. Thermodynamic equilibrium calculations of Godleski et al. [16] and Stein [17] find that such low molecular weight hydrocarbons are not stable in the high temperature (> 600C), reducing environment used to grow CVD diamond. Stein [17] finds that the favorable enthalpies of formation of such diamond forming precursors as adamantane, diadamantane and cyclohexane are overwhelmed by unfavorable entropies of reactions above 500 K. Above this temperature, the corresponding graphite precursors (polycyclic aromatics) are found both theoretically and experimentally to be more stable. In addition, below this temperature calculations show these diamond-like molecules to be unstable with respect to dissociation into methane and other small molecular weight gas species.

Angus et al. [18,19] have, in turn, proposed various saturated multiple fused ring compounds (with structures representative of nascent parallel twin planes of diamond) as possible diamond precursors. Such "graphite precursor" as described in the hydrocarbon flame and combustion literature [20, 21], are stable in the high temperature reducing atmosphere of CVD diamond growth. However, no published reports have appeared of successfully using such aromatics to nucleate diamond. On the contrary, Frenklach and Wang [22], in a detailed chemical kinetics model of a hot filament CVD reactor, find that in the operating parameters typical for diamond deposition, atomic hydrogen suppresses the formation of such aromatics.

More recently, Shen et al. [23] have modelled diamond based

precursors employing a finite cluster approximation approach. This theoretical model investigates carbon cluster fragments of the diamond lattice which are saturated by hydrogen atoms, so called adamantane based or polymantane derived carbon clusters. Ab initio quantum mechanical computations are used to investigate the convergence behavior of the properties of the clusters toward the properties of bulk diamond. Although stable polymantane based clusters of up to only $C_{35}H_{36}$ are calculated and little reference is made to the stability of such molecules in the CVD environment used to grow diamond films, the approach to the problem has much relevance to the results described in this report.

Several detailed studies on the nucleation mechanism of diamond on silicon and metal surfaces have been reported recently. Stoner et al [24] have made an in depth study of diamond nucleation on silicon using a biasing technique developed by Yugo et al [10] in which a negative potential is applied to the substrate with respect to the plasma to enhance carbon ion bombardment of the surface during the nucleation stage. The carbon ions are found to initially form an amorphous silicon carbide layer on the substrate surface. However, continued carbon ion bombardment results in preferential etching of the silicon from the Si-C layer and/or continued high flux of carbon to the surface. This excess carbon is postulated to form small "clusters" favorable for diamond nucleation. The molecular or structural arrangement of such carbon sites is not described.

Belton and Schmieg [25] have studied the nucleation of diamond on

platinum and nickel substrates using hot filament chemical vapor deposition and have elucidated nucleation site structural information. In these experiments, a combination of X-ray photoelectron spectroscopy, electron energy loss spectroscopy, and low energy electron diffraction was used to examine the time evolution of surface carbon species during diamond growth. These results indicate that diamond nucleates on platinum and nickel by pre-deposition of graphitic carbon precursors on mechanically scratched surfaces. They postulate that defect sites in these graphite deposits contain the nucleation sites for diamond. Ong et al [26] have observed similar results from nucleation and growth of diamond crystals on single-crystal copper surfaces implanted with carbon ions. This study shows that during diamond growth on carbon implanted copper using microwave plasma CVD, a polycrystalline graphite film initially forms on the copper surface. This graphitic layer is found to enhance the nucleation of diamond on copper. This study concludes with a simple lattice model for diamond growth on graphite which is $\langle 111 \rangle_{diamond}$ parallel to $\langle 0001 \rangle_{graphite}$ and $\langle 110 \rangle_{diamond}$ parallel to $\langle 11\bar{2}0 \rangle_{graphite}$.

From these studies one can postulate several necessary conditions which must be met to help enhance diamond nucleation on surfaces: (1) a structured, pure carbon source on the surface is necessary to act as a diamond seed. Pure carbon, from simple thermodynamic equilibrium considerations[21] would be inherently more stable than any hydrocarbon molecule at typical CVD diamond growth conditions; (2) the need for the structured carbon source to be

both air stable to facilitate application and durable enough to withstand to a degree the environment in which plasma enhanced CVD of diamond takes place; (3) the need for the structured carbon source to have steps or ledges to serve as diamond nucleation sites; and (4) finally, to have a means of initiating diamond nucleation from the gas phase during the CVD process.

Advances by Kraetschmer et al [27] in the synthesis of gram scale quantities of air stable pure C_{60} and C_{70} and other even larger fullerenes now enable the practical experimental study of the utility of carbon clusters as diamond nucleating agents. In addition to fulfilling the requirements stipulated above for a good diamond nucleating agent, C_{60} and C_{70} clusters are unique from other types of carbon precursors previously studied in two other major respects. The fullerenes are a highly ordered allotrope of pure carbon which is easily formed into thin solid films by a simple low temperature sublimation process. Unlike many proposed hydrocarbon based diamond precursors, these cluster solid films are also found to be chemically stable up to the temperatures at which diamond is found to grow. C_{70} in particular, has a sublimation temperature approaching 600°C, which is a typical low temperature limit for CVD diamond synthesis. We report in this paper the results of attempts to enhance the nucleation of diamond on substrates with the use of C_{60} and C_{70} fullerene films.

III. Experimental Procedure

A. Description of Microwave Plasma CVD Reactor

A microwave enhanced plasma chemical vapor deposition system was designed and constructed for the purpose of depositing high purity diamond thin films. A schematic of the deposition system is shown in Figure 1. The microwave energy operating at a frequency of 2.45 GHz is directed to the CVD reactor through a circular waveguide, then launched into the chamber through a quartz window. The substrate holder consists of a quartz tube with an annular cap, which is used to keep the sample in place. The cap is made of either graphite, quartz, or boron nitride depending on the particular experiment. In this configuration the sample is floating with respect to the plasma when no bias potential is applied. Bias with respect to the plasma is made via platinum foil in mechanical contact with the back of the sample.

B. C_{60} and C_{70} Separation and Their Properties

Purified forms of C_{60}, C_{70}, their various derivatives and other higher number carbon clusters were prepared by Shengzhong Liu in the Department of Chemistry at Northwestern University. C_{60} and C_{70} were obtained from carbon soot, prepared by graphite evaporation in a helium atmosphere [28,29] . The clusters were first recovered from the soot by soxlet extraction. Separation of the C_{60} and C_{70} clusters was achieved by dispersing the extracted material on top of a column of active alumina, and eluting with hexane, 5% toluene in hexane, and finally 20% toluene in hexane [30] . The purity of the resulting C_{60} and C_{70} fractions was confirmed by electron impact mass spectroscopy, which showed the C_{70} fraction slightly (< 15%)

contaminated by C_{60}. A comprehensive Raman and IR spectroscopic analysis has also been made of the C_{60} and C_{70} materials produced and is reported elsewhere. [31]

Both the molecular and room temperature lattice structures of C_{60} and C_{70} clusters have been extensively characterized [32,33] . It is known that C_{60} has the form of a truncated icosahedron (I_h) and packs in an FCC lattice (a_o = 1.42nm.). The more familiar model of the 12 pentagonal and 20 hexagonal faces of the icosahedron is that of a soccer ball (see Figure 2a.).

C_{70} has a hexagonal closed packed lattice arrangement at room temperature (a = 1.01nm and c= 1.68 nm). The C_{70} molecular structure is not yet rigorously characterized. However, there is extensive ancillary evidence supporting a proposed D_{5h} symmetry [34] . In C_{70} 12 pentagonal and 25 hexagonal carbon rings form a rugby-ball, egg shaped cage (see Figure 2.b). Ten of the twelve pentagons are symmetry equivalent and only two of them (top and bottom, perpendicular to the c-axis) are regular [35] (Manolopoulos et al. 1991). Scuseria et al. [36] , using ab-initio self-consistent field (SCF) Hartree-Fock computations to calculate equilibrium atomic distances, find three categories of bonds: single, aromatic, and double bonds in C_{70}. The double and intermediate bond lengths are slightly longer than the typical double (1.33Å) and aromatic (1.39Å) C-C bonds. Although at first glance the structure of C_{70} seems very different from that of C_{60}, they are, on closer inspection, quite similar. The extra ten carbon atoms in C_{70} are located in a central loop in the xy plane, which gives rise to an

additional band of five aromatic hexagonal rings. The top and bottom of the cluster remain the same as C_{60}.

IV. Fullerene Nucleation Enhancement Experiments

All cluster nucleation experiments were conducted on (100) p-type boron doped Si wafers (resistivity of 1.8-2.4 ohm-cm). The silicon substrates were first cleaned in acetone and methanol, then boiled for ten minutes in nitric acid at 130°C. The samples were next etched in 40% hydrofluoric acid before being loaded into the evaporator for the C_{60}/C_{70} cluster sublimation. The clusters were sublimated onto the silicon substrates either as continuous films or (through a shadow mask consisting of) an array of 200 micron diameter dots. By this latter masking procedure, several important experimental controls were simultaneously established. In the form of 200 micron diameter islands, the cluster film thickness could be easily measured with a profilometer. Since the sample contains regions of covered and exposed Si, the nucleation of diamond on cluster films is able to be compared with that of the Si surface under the exact same plasma processing conditions. Additionally, since the substrate contains a large array of cluster dots, any plasma nonuniformity or sample edge effects on nucleation can be identified.

A series of C_{60}/C_{70} cluster array samples were prepared with varying cluster thicknesses from 20 nm to 2 microns. The above cluster films did not enhance diamond nucleation on Si substrates

over a wide range of typical diamond growth conditions. Diamond was found to nucleate substantially on C_{70} cluster films only after a pretreatment was performed on the cluster arrays. This pretreatment consisted of positive ion bombardment of the C_{70} film on Si by d.c. biasing (-100 to -300 volts) the substrate in a low pressure, low power, hydrogen/methane plasma. During this fifteen minute pretreatment, the gas composition is 10% methane in H_2 at a pressure of 15 torr, flowrate of 100sccm and input microwave power of 400 watts. After this pretreatment, normal diamond growth is initiated on the sample.

Figure 3.a shows a scanning electron micrograph of diamond growth on an array of 100nm thick C_{70} dots on Si with a closer view of an individual dot in figure 3.b. Figure 3.c shows the grain size and morphology of the continuous diamond film nucleated on the dot. The nucleation density of diamond particles is found comparable to that obtained on diamond polished Si substrates under similar plasma growth conditions (see Figure 4). The procedure also works for continuous films of C_{70} on Si. Figure 5.a shows the an SEM micrograph of a continuous diamond film grown over an entire Si substrate which was initially coated with a 100nm thick C_{70} layer. The substrate was pretreated with the same conditions used on the C_{70} arrays prepared on Si substrates (see Figure 3). Figure 5.b shows the corresponding Raman spectrum of the continuous film confirming that the nucleated phase is indeed diamond.

The bias pretreatment which activates the C_{70} clusters for diamond nucleation was found to be strongly influenced by several

deposition conditions. Negative biasing implies that ion bombardment by positively charged plasma species on the C_{70} surface is necessary to initiate diamond nucleation. The energy at which these charged species impinge on the cluster film surface is determined by their acceleration across the sheath potential which is formed between the substrate and the plasma. The charged species are accelerated to energies given by $E_s = e(V_{substrate} - V_{plasma})$, where V_{plasma} is the plasma potential with respect to ground, and $V_{substrate}$ is the substrate voltage relative to ground. The magnitude of E_s thus depends on the difference between the applied d.c. bias relative to plasma potential. It is also influenced by several interrelated (dependant) variables which include the gas pressure, the input microwave power coupled into the discharge, and the impedance and dimensions of the substrate/substrate holder. In addition to the above electric field dependant parameters, several other variables influenced the cluster bias activation, such as the C_{70} film thickness, the methane concentration in the discharge during biasing, and the duration of biasing.

The parameter "window" for effective activation of the C_{70} clusters was found to be fairly narrow. Before one can analyze the influence of the above mentioned variables on the bias pretreatment, the degree of diamond nucleation enhancement on the Si substrate which signifies that the cluster film has been successfully activated needs to be clarified. In general, for different bias pretreatment conditions, the degree of nucleation enhancement showed considerable variation. In certain cases, after

bias pretreatment, diamond crystallites would preferentially nucleate on a C_{70} dot but not to a density comparable to that usually obtained on diamond polished substrates. For other conditions, substantial nucleation would occur on cluster film dots only in narrowly defined areas of the substrate. In the following discussion, successful C_{70} bias activation will imply that diamond has nucleated on the cluster coated sample with a density similar to that obtained on diamond grit polished substrates. The diamond nucleation enhancement also occurs over a significant area of the substrate surface.

The nucleation density of diamond obtained on the cluster dots was not found to be critically dependant on the C_{70} film thickness. Although a thickness "window" was found for the nucleation enhancement effect in the bias parameter space so far investigated, the grain size in the films was always typically << 1 micron for a wide range of cluster film thicknesses. Diamond nucleation enhancement was observed for C_{70} films, which range in thickness from 20nm. to 400nm. The accurate measurement of cluster film thicknesses below 20nm precludes the extensive experimental investigation of enhancements below this level.

The influence of cluster film thickness on nucleation enhancement is clearly demonstrated when comparing thickness profiles of C_{70} dots before pretreatment/diamond growth and the resulting SEM micrographs of the nucleated diamond films (see Figure 6). The cluster films produced by sublimation have very non-uniform thicknesses. Limited amounts of initial cluster solids

necessitate placement of the substrates very close to the evaporation boat during the sublimation step to produce the carbon cluster films/arrays. This results in very non-uniform thickness profiles across the substrate surfaces. Typically, on substrates placed directly above the evaporation boat, uniform films are produced (Figure 6.b) while substrates further from the epicenter have less uniform coatings (Figure 6.a,c). Figure 6.c shows the thickness profile across a C_{70} dot with a maximum height of 400 angstroms which tapers off across the layer. Such a profile is typical for many of the dots on the silicon substrate. Alongside the thickness profile is an SEM micrograph of the resulting nucleated diamond film on one of the 400A thick C_{70} dots. The nucleation density of diamond on the dot decreases as the C_{70} layer thickness becomes thinner. From such profiles one estimates a minimum cluster thickness of 200A is needed to effectively nucleate diamond with the pretreated processing parameters so far investigated.

Figure 6.a shows the profile for one of the thicker C_{70} arrays tested with its corresponding nucleated diamond film shown in the SEM micrograph to the right. In this case no nucleation enhancement is found in the thicker regions of the C_{70} film with the result that a large hole is produced in the final diamond film. It is believed that this phenomenon results from too short an activation time for the thicker cluster films. Time lapse Raman measurements of the cluster films during different stages of the pretreatment show that the C_{70} layer is slowly being etched/reacted away. It is

believed that only a portion of the C_{70} is being converted into the appropriate diamond precursor on the surface of the film while the rest is sputtered/reacted off the silicon substrate. After 15 minutes of bias pretreatment, what mostly remains on the surface of the Si substrate is appropriate diamond precursor. However, for the thicker samples not all of the C_{70} film is totally converted into the diamond precursor after fifteen minutes of pretreatment. An underlying layer of pure C_{70} still remains beneath an activated layer of C_{70}. When normal diamond growth is next initiated on the substrate, the temperature rises above 650°C. At this temperature the underlying C_{70} layer sublimates off of the substrate carrying away the activated layer on its surface. This surface activation model also explains why the grain size in both 400A and 4000A films are comparable since only the exposed surface area of the cluster film is being converted.

For a methane concentration of 1% in hydrogen, the C_{70} clusters films were not activated to enhance diamond nucleation. In the range of 10-20% methane in hydrogen, the cluster films became activated. At higher methane concentrations black soot was deposited onto the cluster surface during the bias activation step. The above concentration dependance results are consistent with previous studies on methane/hydrogen plasmas. A global chemical reaction model recently developed by Frenklach and Wang [22] for the methane hydrogen gas system is useful for interpreting the above observations. This model incorporates experimental data on the composition and chemical reaction mechanism in the activated

hydrocarbon/hydrogen system from a large number of published sources. The chemical reaction kinetics occurring in an activated methane/hydrogen gas system in contact with a surface are fairly complex in which a large number of competing chemical reactions can be described. To simplify the discussion Frenklach and Wang divides the gas phase species in the system into two categories; diamond forming reactants and graphite precursors. The methyl and C_2H_x species (acetyl, vinyl, ethylene, ethyl and ethane) are important for the diamond forming mechanism. The corresponding graphite precursors are gas phase benzene derivatives and other aromatic and polycyclic aromatic hydrocarbons (PAH). The plasma environment consists of a competition between condensation of sp^3 (important for diamond nucleation) and sp^2 (aromatic) species, gas phase and surface site chemical conversion of sp^2 to sp^3 species and vice versa, as well as gasification of both products by atomic hydrogen.

Studies find for low methane concentrations, the gasification rate of aromatic species deposited on a surface is greater than their corresponding rate of condensation from the gas phase. At low methane concentrations the formation rate of benzene derivatives necessary for the gas phase synthesis of PAH is also further suppressed. This results in a gas phase composition which is predominately C_2H_x and methyl species. With the increase of methane concentration in the plasma, the gasification rate of carbon species by atomic hydrogen decreases, while the formation rate of PAH in the gas phase increases. Eventually, the condensation of PAH (soot) from the gas phase is the predominate reaction in the

system. This coverage of soot deactivates all surface related chemical processes.

The C_{70} films are not activated for methane concentrations of 1% because, with the substrate surface biased, the dominant reaction is gasification of carbon species (the C_{70} film included) by atomic and various hydrogen radicals. Since the C_{70} film surface is being constantly removed, there is no stable site for chemical modification of the cluster. For methane concentration between 10-20% the percentage of important methyl and C_2H_x species increases in the gas phase while the etching rate of atomic hydrogen decreases. This regime allows for surface modification of the cluster film. The details of this mechanism are described in section V. With higher methane concentrations the condensation of benzene derivatives predominates. Since the formation of PAH is largely a gas phase reaction process, the nature of the surface in contact with the plasma is irrelevant. Soot will be deposited on any surface at the higher methane fractions. The above argument is similar to that applied to the growth of diamond films at higher temperatures (600-1000°C) from activated methane/hydrogen gas mixtures. However, the methane concentration dependance for the C_{70} cluster activation is shifted to higher values (10%) than for the diamond growth case (1%). This is believed to be due to the enhanced reaction kinetics induced by the applied dc bias, which shifts important etching/deposition reaction rates.

To verify that the nucleation enhancement observed was due specifically to the presence of the cluster film and would nct

occur with any carbonaceous material subjected to the same pretreatment, a series of diamond nucleation and growth experiments were performed with other types of carbon films. Figure 7 shows the Raman spectra for the various carbon materials tested. Figure 8 shows the SEM results after the same bias pretreatment and diamond growth (under the same deposition conditions) on the series of samples for comparison. As Figure 8 clearly shows, all the various types of carbon tested enhance nucleation to some degree compared to the untreated Si substrate. This result is not surprising. Such an effect has been reported by previous researchers [9, 37, 38]. Most of the carbon films investigated, as distinguished by their Raman spectra, are graphitic in nature but have a high degree of atomic disorder (with the exception of the C_{60} and C_{70} films and the HOPG substrate). Earlier studies have identified lattice planes in graphite conducive to diamond nucleation [18,26]. It is not surprising that a disordered graphitic state would statistically contain a range of kinetically favored sites for diamond nucleation. What is of significance is the much greater diamond nucleation enhancement of the C_{70} film compared to that of the other carbon materials, even to that of C_{60}.

Figure 8.b shows the SEM micrograph for diamond grown on a 1000A thick, bias pretreated C_{60} dot while its corresponding Raman spectrum is found in Figure 7.b. Although an enhancement in nucleation is also found for C_{60} dots, it never approaches the degree of that of the 1000A thick C_{70} dot, which is shown in Figure 8.a. It was initially expected that C_{60} would be a better nucleation

precursor than C_{70}. The molecule is considered more stable than C_{70} and recent HRTEM [33] as well as X-ray diffraction results [32] confirm an FCC packing arrangement in the cluster film. Possible reasons why C_{60} is not as good a diamond nucleation promoter as C_{70} will be discussed below.

Figure 8.c shows the SEM results of a comparison of C_{70} nucleation enhancement to that of a DLC amorphous coating of comparable thickness grown on the same substrate. Figure 7.c is the Raman spectrum of the deposited DLC film. For this series of experiments C_{70} dots of various thicknesses were sublimated onto Si substrates. Next, an amorphous diamond like coating was deposited on the exposed Si surface between the cluster films.

The DLC/C_{70} samples were prepared as follows. C_{70} was first sublimated onto cleaned (100) Si substrates through the 200μm dot shadow mask. These substrates were then placed in a capacitively coupled RF CVD reactor wherein a 1000A DLC film was deposited from an argon/methane gas mixture operating at 35mtorr and 25 watts of power. During these initial amorphous carbon film depositions, it was discovered that the DLC coating adhered well to the exposed Si surface but did not stick to the surface of the C_{70} cluster films. Over time, blisters appeared on the DLC film covering the cluster dots. After a few hours of exposing the sample in air, the blistered DLC overlayer peeled completely from each dot exposing the underlying cluster layer.

For the case of the C_{70}/DLC samples no significant enhancement in diamond nucleation was found in the areas of the substrate

coated with DLC (see figure 7.c) while substantial growth is found on the cluster dot region. The nucleation enhancement on the C_{70} dots, though, was not as high as that found for C_{70} films which were not coated with DLC layers. This diminished enhancement was discovered to be due to the destructive argon ion bombardment sustained by the cluster film during the RF plasma deposition of the DLC layer.

An amorphous carbon with more graphitic features as discerned from Raman analysis was also tested of which the results are depicted in Figure 8.d. Figure 7.d shows the Raman spectrum of the corresponding carbon film. Dots of this amorphous carbon film were prepared by evaporating graphite (arc melt) through a shadow mask onto Si substrates at a base pressure of 10-6 torr using a standard carbon rod sputtering attachment in an evaporator. In this case, again a slight enhancement in diamond nucleation is found, but not to the degree of C_{70} dots.

A more structured graphitic material similar to polycrystalline graphite was also tested. This sample was prepared by arc melting graphite in helium at 200 torr of pressure. Again, a shadow mask on a Si substrate is used to produce 200 micron diameter dots of soot. Figure 7.e shows the corresponding Raman spectrum of the prepared soot. Soot dots showed the least amount of enhancement of all the dots prepared (Figure 8.e). This result is not unexpected since the soot did not form a very sturdy film. The dots of soot could be easily wiped or even blown off the silicon substrate.

Finally, in another series of experiments, C_{70} dots were deposited onto a highly oriented pyrolytic graphite (HOPG) substrate (Union Carbide). Figure 7.f shows the Raman spectrum of the HOPG substrate, while Figure 8.f the results after plasma pretreatment and diamond growth.

For the case of the C_{70}/HOPG samples very little diamond nucleation was found on the graphite substrates. The areas where diamond did nucleate correspond to the regions where C_{70} dots were sublimated (see Figure 8.f). In this case substantial nucleation was not achieved on the cluster regions because the HOPG surface is too unstable in the hydrogen discharge and is being constantly etched away. The surface underlying the diamond seeds becomes etched away, dislodging the growing diamond crystallite.

Another important observation to note in Figure 8 is the relative areas of enhanced diamond nucleation on the different types of carbon materials tested. All the carbon materials were deposited through a shadow mask consisting of an array of 200 micron dots. Only the C_{70} arrays produced a final diamond coated dot with a diameter comparable to the films' initial 200 micron diameter. The other carbon materials which include the C_{60}, amorphous carbon, and carbon soot dots produce areas of enhanced diamond nucleation considerably less than 200 microns. This phenomena implies that the C_{70} films are less susceptible to hydrogen plasma etching than the other carbon materials. In typical gas phase plasma etching of materials, the edges of a film etch at a faster rate than its surface which thus produces a

gradual shrinkage of the films surface area over time. The smaller diamond dots produced by the other carbonaceous materials imply that carbon etched away from the edges of these 200 micron dots before nucleation of diamond could occur. What is more surprising is that the C_{60} films were found to be more susceptible to hydrogen etching than C_{70} films .

To test the hypothesis that C_{70} films etch at a slower rate in atomic hydrogen than C_{60} ones, the rate of gasification of the clusters in a hydrogen plasma was determined using FTIR spectroscopy. In this experiment equal thicknesses of both C_{60} and C_{70} films were sublimated onto one inch KBr windows . The infrared spectral features of both thin films were recorded. The samples were then placed in an RF plasma reactor. The substrates were next etched in a hydrogen plasma at 500 mtorr for selected intervals after which FTIR spectra were recorded. The samples were tested in the RF discharge to decrease the rate of gasification as compared to the microwave plasma reactor. When no carbon cluster spectral features were discerned by FTIR, the KBr substrate was considered totally etched. The results of this experiment did indeed find the rate of C_{60} gasification to be four times that of C_{70} films.

In conclusion it has been definitively shown that the enhanced diamond nucleation is largely due to the presence of the specific carbon cluster, C_{70} , and is not solely due to the bias pretreatment in the presence of carbon. In addition, the results imply that one factor contributing to the success of C_{70} as a nucleating agent is its stability against hydrogen plasma etching.

The enhancement in diamond nucleation with C_{70} thin films was found to work on other substrates besides Si. Figure 9ab shows an SEM micrograph and Raman spectrum of diamond crystallites nucleated on a quartz substrate which had been pretreated with a C_{70} cluster film layer. The nucleation density is comparable to that obtained on the Si surface with diamond grit pretreatment. C_{70} films were also sublimated onto metals such as molybdenum and tungsten to see if the diamond nucleation enhancement also occurred on these surfaces. Figure 10 shows an SEM micrograph of diamond crystals nucleated on an unpolished molybdenum substrate which was initially coated with a C_{70} cluster film. Enhanced diamond nucleation does occur on the metal surfaces, but it is not to the degree found on the Si or quartz substrates. The lower degree of diamond nucleation on metal surfaces is believed to be due more to their lower resistivity than the semiconductor or insulator substrates. The metal surfaces do not charge up to the degree of the other substrates in the plasma under similar applied dc bias conditions, and consequently will not be subjective to the same level of cation bombardment.

V. Discussion

An appropriate model to explain the enhancement in diamond nucleation must take into account two key points. These points are of importance: 1) negative bias and 2) the specificity of the C_{70} carbon cluster structure for the activation process. The importance

of biasing in the process is treated first.

Because of their low mass, electrons in a plasma respond to electric fields more quickly than the heavier ions. This makes the electrons much more energetic than the ions. Consequently, they are the dominant charge carriers in the plasma. Because of this higher mobility for electrons, they recombine at a much faster rate with the chamber walls than that of the ions, generating a net positive charge in the plasma. A steady state potential called the plasma potential is eventually reached when the rate of loss of electrons to the wall equals the rate of loss for ions. This potential is several volts more positive than that of the chamber potential. If a floating (ungrounded) surface (ie. substrate) is placed in contact with the plasma, it will charge negatively due to the faster rate of bombardment by the more mobile electrons. An equilibrium surface or floating potential (self bias) will arise which will be negative with respect to plasma potential. Since the bulk plasma is of uniform potential, this voltage drop is confined to a thin region above the substrate surface, called the plasma sheath. Electrons are further accelerated across the sheath making this area of very low electron density. With fewer electrons, a reduced number of radiative recombination occurs making the sheath region above the substrate appear "darker" than the rest of the plasma.

The influence on thin film deposition of the width and electric field intensity of the plasma sheath is well documented in the Plasma Enhanced CVD literature [39,40,41] . The activation of

plasma deposition processes by manipulation of the sheath through external biasing has also been well demonstrated for a variety of thin film material systems [42,10].

A recent study on the importance of the substrate bias for nucleation phenomena in plasma CVD has particular relevance to the present work. Vandentop et al. [41] have investigated the initial stages of amorphous carbon deposition on Si and graphite substrates in an RF (13.56 MHz) parallel plate reactor operating at 65 mtorr. Scanning tunnelling microscopy was used to monitor the early growth kinetics of carbon deposition on the substrates. The key finding is that for the graphite samples, amorphic, 50A diameter, carbon clusters nucleate and coalesce into a hard film only when the substrate is placed on the negative electrode of the reactor. At this electrode a self bias or sheath voltage of 350V is estimated compared to approx. 15V on the grounded electrode. When the graphite sample is placed on the grounded electrode, only soft polymer like films are deposited. Since the flux of neutral radical species to both electrodes is about the same, one concludes that high energy cations are important for the initial amorphic cluster nucleation phenomena.

The ideal graphite surface, fully terminated is relatively unreactive. The sticking probability of methyl radicals to its surface is estimated to be very low. An initial disruption to the carbon bonding is necessary before CH_3 radicals can link to this surface. From Vandentop's analysis, this disruption on the surface is provided by high energy methyl cations bombarding the substrate,

which is situated on the self biased electrode. Irreversible bonding of a radical species next occurs at an ion induced defect, which quickly grows into a 50A size cluster.

The above arguments of Vandentop et al. [41] can similarly be used to explain why it is necessary to bias the substrate to activate the C_{70} molecule for diamond nucleation. The cluster's cage like structure, for the present analysis, can be loosely thought of as closed graphitic sheets. Recent ion beam scattering [43] and laser ionization [44] studies on C_{60}, C_{70}, and C_{84} find these carbon clusters to be both highly resilient to impact fragmentation and also chemically inert. Such results are consistent with the closed, edgeless, spheroidal shell structure of the molecules. To modify the surface of the cluster in a plasma, it is reasonable to assume that the first necessary step is some type of energetic disruption of the closed shell bonding.

The similarity in the unreactive nature of the C_{70} cluster film surface in a methane plasma compared to that of graphite substrates has been previously alluded to. In that case, DLC layers were deposited on Si substrates coated with an array of C_{70} dots. The DLC layer was found to stick very well to the exposed portion of the Si substrate but not to the C_{70} regions of the film. The carbon films deposited on the C_{70} dots were soft and easily delaminated from the cluster surface just as in the case of Vandetop's graphite substrates on the grounded electrode. Though the C_{70} coated substrate was placed on the self biased electrode, the small RF powers (25 watts) used during the DLC deposition produced a self

bias much less than the 350 V found necessary in Vandentop's work.

A simple estimate can be made of the single plasma ion energy necessary to break one carbon cluster bond in a C_{70} molecule. This value can then be compared to a typical floating substrate potential obtained in the microwave plasma CVD system at the conditions used to grow diamond films. The C_{70} cluster has 105 bonds of which 70 are single and 35 are double. Since bond energy values for the C_{70} molecule have not as yet been calculated or measured, an approximate figure of 348 kJ/mole is assumed for a single carbon-carbon bond and 614 kJ/mole for a double one [45] . If the impinging plasma cation dissipates its energy upon impact over all bonds in the molecule, an energy of approximately 475 eV is necessary to assure one bond is broken.

An estimate is now needed of the floating potential of the substrate without the application of a dc bias in the present microwave plasma system. One can calculate the floating potential and sheath width for a plasma from the Langmuir probe theory using the Childs-Langmuir equation. However, this relation is derived for the case of a low pressure (<< 1 torr), cold discharge in which a basic assumption is that acceleration of ions across the sheath are collisionless [39]. This assumption does not hold for the pressures used to activate (15 torr) the clusters or grow diamond films (above 1 torr) with a microwave discharge where electron-neutral, ion-neutral collisions dominate. In this pressure regime the plasma is in a transition between an ambipolar diffusion controlled discharge and a free floating microwave arc [46] . Simple analytical

expressions have not as yet been developed to describe these systems.

From simple plasma discharge principles, an approximate floating potential can be deduced. Unlike dc and rf plasmas, microwave discharges are sustained without the use of electrodes. Therefore, their is no clearly defined anode or cathode. The sheath widths on surfaces in contact with the discharge are quite thin on the order of tens of microns. Since the substrate is also floating, its potential will not be that much greater than plasma potential. Zhang et al. [46] have measured the electric field intensity of a microwave plasma in a reactor of similar design to the present system. This intensity was measured as a function of the typical pressure, power, and gas compositions used to grow diamond films. For a pressure of 15 torr and input microwave power of 400 watts, Zhang et al. find an absolute electric field intensity of 100 V is necessary to sustain the discharge. Since the discharge is maintained in a metal chamber, a large potential is not developed between the walls and the plasma. The floating potential of the substrate is thus estimated at about 100 V or less.

This self bias is not large enough to effectively break enough surface bonds in the C_{70} molecule. This explains why pretreating a C_{70} film in an unbiased, hydrogen/methane plasma at 15 torr for 15 minutes does not activate the clusters for nucleation. With the application of an additional negative 200 - 300V bias to the floating substrate, enough kinetic energy is imparted to the cations accelerated across the sheath to break some carbon bonds in

C_{70} to make the molecule more chemically reactive.

The previous simple bond energy arguments only explain why biasing the C_{70} molecule is necessary to impart more chemical reactivity to its surface. A more detailed mechanism is needed of what structural changes are incurred in the molecule which make it activated to nucleate diamond.

A simple kinetic model to explain the bias activated enhancement of diamond nucleation with a C_{70} cluster has been given earlier. This mechanism takes into account several unique structural features of the C_{70} molecule compared to that of C_{60} and other carbon forms. The model is most easily visualized by positioning a C_{70} cluster with its c axis parallel to a horizontal plane. Along the short axis perimeter of C_{70} are five ensembles of four hexagons which, because of their near planar microfaceted structure, are ideal for diamond nucleation.

Figure 11 highlights one such ensemble. In this model energetic cation impact (negative bias) activation results in sp^2 to sp^3 conversion of one of the ensembles followed by its termination with H or CH_3 groupings. Such a restructuring would produce chair-form cyclohexane linkages which are well known to be the most stable six member ring conformation free from strain. These linkages are representative of the surface of the 111 plane of diamond. Onto this C_{70} derivatized hydrogenated/methylated surface, a 111 diamond lattice is then easily propagated.

To further extend this derivatized surface into a single layer diamond lattice it proves helpful to reintroduce the diamond growth

model of Tsuda et al. [47] . Tsuda's growth mechanism has been largely discredited because it relies on a methyl cation for lattice propagation. Although common in methane/hydrogen plasma discharges, this species is not found in any abundance in ion free, hot filament reactors used to grow diamond films. Any growth mechanism for diamond must be applicable to all of the current CVD methods used to deposit this material. The model is useful, though, in extending onto the methylated C_{70} surface created after cation impact, a three dimensional diamond lattice. The first step of Tsuda's model is either methylene insertion or hydrogen abstraction followed by methyl radical addition onto a model compound with a surface representative of the diamond (111) plane. Such a surface is present on the C_{70} cluster after cation impact/ hydrogenation in our model. In the second step, a methyl cation initiates the loss of three H_2 molecules resulting in the simultaneous bonding of three neighboring methyl groups to form the diamond structure (see Figure 12). An enhanced concentration of cations is ensured by the continued application of the external negative bias to this surface. Figure 13 shows the cluster model with a (111) oriented closed diamond cage nucleated on a carbon cluster surface. The minimum energy geometry for this model is calculated with a Force-Field procedure computer program (SYBYL) [48] . Further propagation (ie growth) of this lattice, though, is kinetically hindered because of the low temperature and high methane concentration during the bias activation phase. Extension of the lattice into a macroscopic diamond crystallite is next obtained in the high

temperature/pressure, unbiased, standard growth step used for diamond deposition.

Figure 14 shows extension of the above mechanism in which several C_{70} derived subunits are linked by a (111) oriented diamond sheet in such a way as to roughly conserve the inter C_{70} lattice spacing. Although the above model is highly speculative until further study is completed, the results suggest that oriented films of C_{70} could possibly be used as a buffer layer for heteroepitaxy of diamond on a nondiamond substrate.

The bias enhancement is effective for the C_{70} molecule and not for C_{60} and other forms of carbon for several important structural reasons. The flattened, egg shape of the C_{70} cluster provides a relatively planar surface for nucleation of diamond that ensures closure of a number of diamond "cages" without major lattice distortion. The high surface curvature of the C_{60} cluster is not conducive in this respect to propagation of a diamond lattice sheet. C_{60} also does not have a grouping of four fused hexagonal rings which serve to "lock in" a diamond lattice structure on the surface of the cluster. Another important feature of the C_{70} cluster different from other solid forms of carbon is the hollow shell structure which provides an inner and outer surface for chemical kinetics. A graphite solid, the closest analog to the cluster structure, has only one reaction surface. The C_{70} cage structure also aids nucleation because it provides a nonrigid surface which will relax to relieve any stress generated by bond angle strain between the nucleated diamond sheet and the carbon cluster base.

To further elucidate the chemical mechanisms occluding during the bias pretreatment process, Raman and IR measurements were performed on a series of C_{70} coated Si substrates which were subjected to different stages of bias activation. By monitoring the activation stage at different time intervals it was hoped that some aspects of the proposed model could be substantiated. Unfortunately, no in-situ IR or Raman spectroscopy analysis is possible in the current plasma CVD system. The pretreated samples were exposed to air before measurements could be made. Early observations found that once the pretreated cluster covered substrate was exposed to air and then returned to the deposition system for subsequent diamond growth, the nucleation enhancement was sharply reduced. Further work is needed to understand this effect. Efforts are underway to incorporate an in-situ Raman spectroscopy capability into the present deposition system and will be reported on at a later time.

VI. Conclusions

In summary, the enhancement in diamond nucleation with C_{70} cluster films is found to be generally applicable to CVD diamond growth on metals, semiconductors, and even insulators. The enhancement effect is shown to be specific to the C_{70} carbon cluster and is not produced in other forms of pure carbon under similar biasing conditions. The bias activation step is also found to be critically dependent on the processing parameters of pressure,

power, methane concentration, cluster film thickness , and substrate conductivity.

In this paper a unique method for nucleating diamond films on smooth surfaces has been developed. This process substitutes the need for diamond grit polishing pretreatment of substrates prior to film growth as currently practiced in low pressure (< 1 atm.), CVD methods used to produce diamond films. A thin solid film of C_{70}, sublimed onto a Si surface, is found to significantly enhance the nucleation of diamond on this material in a microwave plasma discharge after a critical activation step.

Before the cluster film will promote diamond nucleation, a pretreatment is found necessary to chemically activate the C_{70} surface. This activation stage consists of negatively biasing (-200 - -300V) the C_{70} film in a low power, hydrogen/methane (10%) microwave plasma before diamond growth is initiated. The bias activation step is critically dependant on not only the applied dc voltage but also several plasma processing parameters such as pressure, power, methane concentration, cluster film thickness, and substrate conductivity.

The degree of nucleation enhancement obtained is shown to be comparable to that obtained on diamond grit polished surfaces. This diamond nucleation enhancement phenomenon with a C_{70} cluster film is also found to be generally applicable to CVD diamond growth on metals (molybdenum and tungsten), semiconductors (Si), and insulators (quartz). It thus follows that these carbon clusters could be of general use in the optical, electronic and protective

coating applications of diamond thin films.

The successful application of a carbon cluster to diamond nucleation opens a new avenue of investigation in CVD diamond research. In this paper only two types of carbon clusters were investigated, C_{60} and C_{70}. With improved separation procedures, other higher number clusters (C_{78}, C_{84}, C_{92}) and their derivatives ($C_{70}O$) can also be obtained. One can envision using these variable size clusters as nucleation probes to further study the kinetics of the CVD diamond growth phenomenon.

Acknowledgement

This research was supported by the Department of Energy under contract number DE-FG02-87ER45314 and the Office of Naval Research. This work made use of MRL central facilities supported by the National Science Foundation, at the Materials Research Center at Northwestern University, under award number DMR-9120521.

*Grumman Corp., A01-26, Corp. Research Center,
Bethpage, NY 11714-3580

VII. References

1. Koizumi, S. and Inuzuka T., J. Cryst. Growth **99**, 1188 (1990)

2. Kamo, M., Sato, Y., Matsumoto, S. and Setaka, N. J. Cryst. Growth, **62**, 642 (1983)

3. Matsumoto, S., Sato, Y., Kamo, M. and Setaka, N., Jpn. J. Appl. Phys., **21**, Li83 (1982)

4. Hirose, Y. and Kondo, N., Japan Applied Physics Society Meeting, March 29, 1988.

5. Mitsuda, Y., Yoshida, T. and Akashi, K., Rev. Sci. Instrum., **60**, 249 (1989).

6. Meilunas, R.J., Chang, R.P.H., Liu, S., and Kappes, M. M., Appl. Phys. Lett. **59**, 3461 (1991).

7. Yarbrough, W.A., Inspector, A., and Messier, R., Mat. Sci. Forum, **52**, 151 (1989).

8. Iijima, S., Aikawa, Y., and Baba, K., Appl. Phys. Lett., **57**, 2646 (1990).

9. Ravi, K.V. and Koch, C.A., Appl. Phys. Lett. **57**, 348 (1990).

10. Yugo, S., Kanai, T., Kimura, T., and Muto, T., Appl. Phys. Lett. **58**, 1037 (1991).

11. Rudder, R.A., Hudson, G.C., Posthill, J.B., Thomas, R.E., and Markunas, R.J., Appl. Phys. Lett. **59**, 791 (1991).

12. Yehoda, J.E., Fuentes, R.I., Tsang, J.C., Whitehair, S.J., Guarnieri, C.R., and Cuomo, J.J., Appl. Phys. Lett **60**, 2865 (1992).

13. Geis, M.W., private communication (1991).

14. Meilunas, R.J., 1987, *unpublished results*

15. Matsumoto, S. and Matsui, Y., J. Mater. Sci. **18**, 178 (1983).

16. Godleski, S.A., Schleyer, P.V., Osawa, E., Wipke, W.T., Prog. Phys. Org. Chem. **13**, 63 (1981)

17. Stein, S.E., Nature, **346**, 517 (1990)

18. Angus, J.C., Buck, F.A., Sunkara, M., Grot, T.F., Hayman, C.C., and Gat, R., MRS Bulletin **14**, 38 (1989).

19. Angus, J.C., Sunkara, M., Hayman, C.C., and Buch F.A., Carbon **28**, 745 (1991).

20. Stein, S.E. and Fahr, A., J. Phys. Chem. **89**, 3714 (1985).

21. Stein, S.E., J. Phys. Chem. **825**, 566 (1978).

22. Frenklach, M. and Wang, H., Phys. Rev. B **432**, 1520 (1991).

23. Shen, M., Schaefer, H.F., Liang, C., Lii, J., Allinger, N.L., and Schleyer, P.R., J. Am. Chem. Soc. **114**, 497 (1992).

24. Stoner, B.R., Ma, G.H.M., Wolter, S.D., and Glass, J.T., Phys. Rev B. **45**, 11067 (1992).

25. Belton, D.N., and Schmieg, S.J., J. Appl. Phys. **66**, 4223 (1989)

26. Ong, T.P., Xiong, F.L., and Chang, R.P.H., Appl. Phys. Lett., **60**, 2083 (1992)

27. Kratschmer, W., Lamb, L., Fostiropowlos, K. and Huffman, D., Nature **347**, 354 (1990).

28. Kratschmer, W., Fostiropoulos, K. and Huffman, D., Chem. Phys. Lett. **170**, 167 (1990).

29. Whetten, R.L., Alvarez, M.M., Anz, S.J., Schriver, K.E., Beck, R.D., Diederich, F.N., Rubin, Y., Ettl, R., Foote, C.S., Darmanyan, A.P., and Arbogast, J.W., (1991) in Clusters and Cluster-Assembled Materials, Mat. Res. Soc. Symp. Proc. **206**, in press.

30. Aje, H., Alvarez, M., Anz, S., Beck, R., Diederich, F., Fostiropoulos, K., Huffman, D., Kratschmer, W., Rubin, Y., Schriver, K., Sensharma, D., and Whetten, R. J., Phys. Chem. **94**, 8630 (1990).

31. Meilunas, R.J., Chang, R.P.H., Liu, S., and Kappes, M. M., Appl. Phys. Lett. **70**, 1 (1991).

32. Liu, S., Lu, Y., Kappes, M.M., and Ibers, J.A, submitted to Science (1991).

33. Dravid, V., Liu, S., and Kappes, M.M., Chem. Phys. Lett. in press (1991).

34. Johnson, R.D., Meijer, G., Salem, J.R., and Bethune, D.S., J. Am. Chem. Soc. **113**, 3619 (1991).

35. Manolopoulos, D.E., May, J.C., and Down, S.E., Chem Phys. Lett. **128**, 105 (1991).

36. Scuseria, G.E., Chem. Phys. Lett. **1805**, 451 (1991).

37. Badzian, A.R. and Badzian, T., in Extended Abstracts: Diamond and Diamond -Like Materials Synthesis, edited by Johnson, G.H., Badzian, A.R., and Geis, M.W., Mater. Res. Soc., Pittsburgh, PA. pg 27. Badzian, A.R., Badzian, T., Roy, R., Messier, R. and Spear, K.E. Mat. Res. Bull. **23**, 531 (1988). Badzian, A. and DeVries, R.C., Mater. Res. Bull. **23**, 385 (1988).

38. Angus, ACS Diamond Meeting, Spring 1990, Washington, D.C.

39. Chapman, B., Glow Discharge Processes, Wiley, New York (1980).

40. Suzuki, K., Okudaira, S., Sakudo, N., Kanomata, I., J. J. Appl. Phys. **16**, 11 (1979).

41. Vandentop, G.J., Nascente, P.A.P., Kawasaki, M., Ogletree, D.F., Somorjai, G.A., and Salmeron, M., J. Vac. Sci. Tecnnol. **A9**, 2273 (1991).

42. Vossen, J.L., J. Vac. Sci. Tech. **8**, S12 (1971).

43. Beck, R.D., St. John, P., Alvarez, M.M., Diederich, F., and Whetten, R.L., J. Phys. Chem. in press (1991).

44. Zhang, Q.L., O' Brien, S.C., Heath, J.R., Liu, Y., Curl, R.F., Kroto, PH. W., and Smalley, R.E., J. Phys. Chem. **90**, 525 (1986).

45. Brown, T.L. and Lemay, E.H., Chemistry, The Central Science, Prentice-Hall, New Jersey pg. 189.

46. Zhang, J., Huang, B., Reinhard, D.K., and Asmussen, J.J. Vac. Sci. Tech. **A8**, 2124 (1991).

47. Tsuda, M., Nakajama, N., and Okawa, S., J. Am. Chem. Soc. **108**, 5780 (1986). J.J. Appl. Phys. **26**, 1527.

48. Liu, S. 1991. unpublished results.

Figure Captions

Figure 1. Schematic of microwave Plasma enhanced CVD reactor.

Figure 2a. Model of C_{60} carbon cluster.

Figure 2b. Model of C_{70} carbon cluster.

Figure 3. SEM micrograph of (a) diamond growth on an array of 100nm thick C_{70} dots, (b) a closeup of an individual, diamond coated 200 micron diameter dot, (c) diamond film grain size and morphology.

Figure 4. Comparison of nucleation density of diamond crystallites grown on (a) a 1000Å thick C_{70} film on Si and (b) an 1/8 micron diamond polished Si substrate.

Figure 5. (a) SEM micrograph of diamond film grown on a C_{70} coated Si substrate and (b) corresponding Raman spectrum of the nucleated film.

Figure 6. Thickness profiles of (a) 8000Å, (b) 1200Å, and (c) 400Å C_{70} dots before bias pretreatment with corresponding SEM micrographs of final nucleated diamond film.

Figure 7. Raman spectra of (a) C_{70} film, (b) C_{60} film, (c) DLC film, (d) evaporated carbon film, (e) carbon soot film deposited on Si substrate and (f) highly oriented pyrolytic graphite (HOPG) substrate. (The Raman band at 520 cm^{-1} is due to the Si substrate.)

Figure 8. SEM micrographs of results of diamond growth on (a) C_{70} dot, (b) C_{60} dot, (c) C_{70} dot/DLC film, (d) evaporated carbon dot, (e) carbon soot dot on Si substrates and (f) C_{70} dot on HOPG substrate.

Figure 9. (a) SEM micrograph of diamond crystallites nucleated on C_{70} coated quartz substrate after bias activation (-250V) and (b) corresponding Raman spectrum of the nucleated layer.

Figure 10. SEM micrographs of diamond crystallites nucleated on a C_{70} coated molybdenum substrate after bias activation (-200V).

Figure 11. Model of C_{70} cluster illustrating one ensemble of four fused hexagonal rings used as a diamond nucleation site.

Figure 12. Reaction mechanism for cation impact generation of diamond lattice from methylated (111) diamond

surface; from (Tsuda, 1986).

Figure 13. Model of (111) diamond nucleation of C_{70} derivative. The minimum energy geometry is calculated with a Force Field procedure using SYBYL.

Figure 14. Photo of a (a) C_{70} model, and (b) (c) simple model consisting of two C_{70} clusters with their surfaces modified to accommodate the nucleation and growth of diamond. The top construction represents a (111) oriented diamond surface. The spheres in the interior represent atomic hydrogen terminating inside the C_{70} clusters.

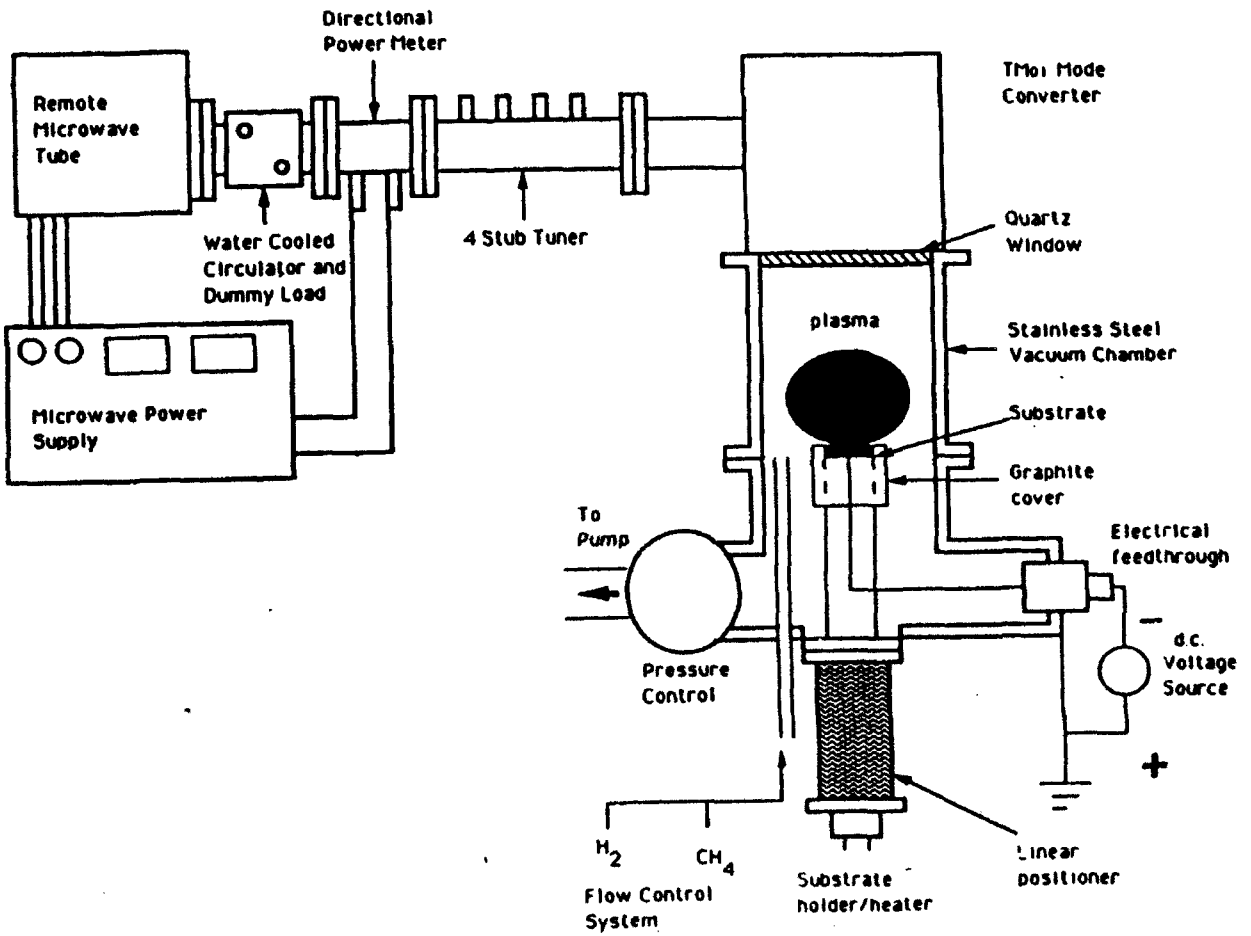
Directional
Power Meter
Remote
Microwave
Tube
TM01 Mode
Converter
Water Cooled
Circulator and
Dummy Load
4 Stub Tuner
Quartz
Window
plasma
Stainless Steel
Vacuum Chamber
Microwave Power
Supply
Substrate
Graphite
cover
To
Pump
Electrical
feedthrough
d.c.
Voltage
Source
Pressure
Control
H_2
CH_4
Flow Control
System
Substrate
holder/heater
Linear
positioner

a.)

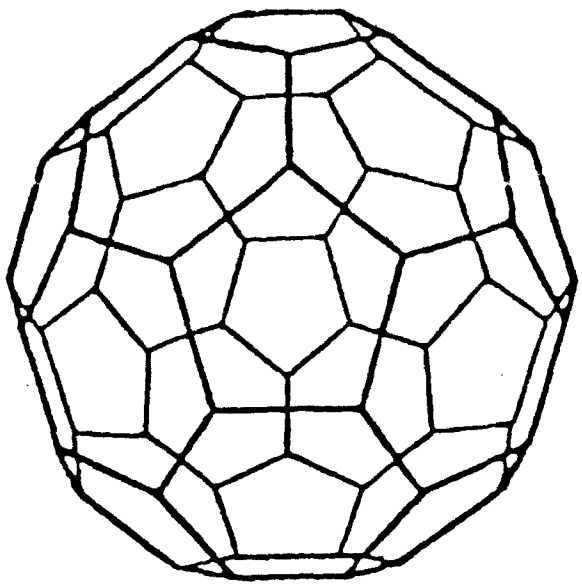

b.)

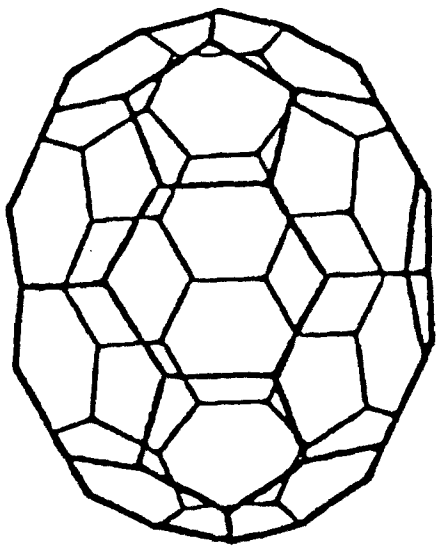

Figure 2a, b

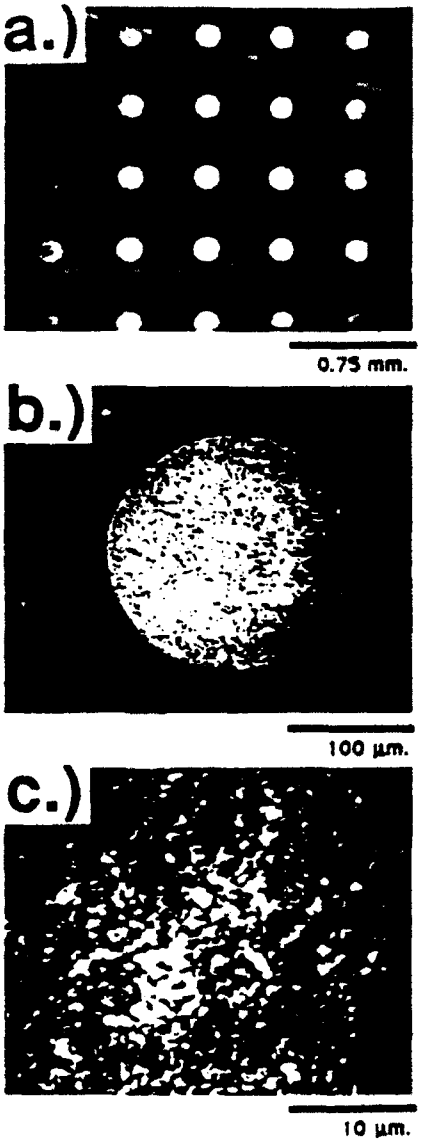

Figure 3

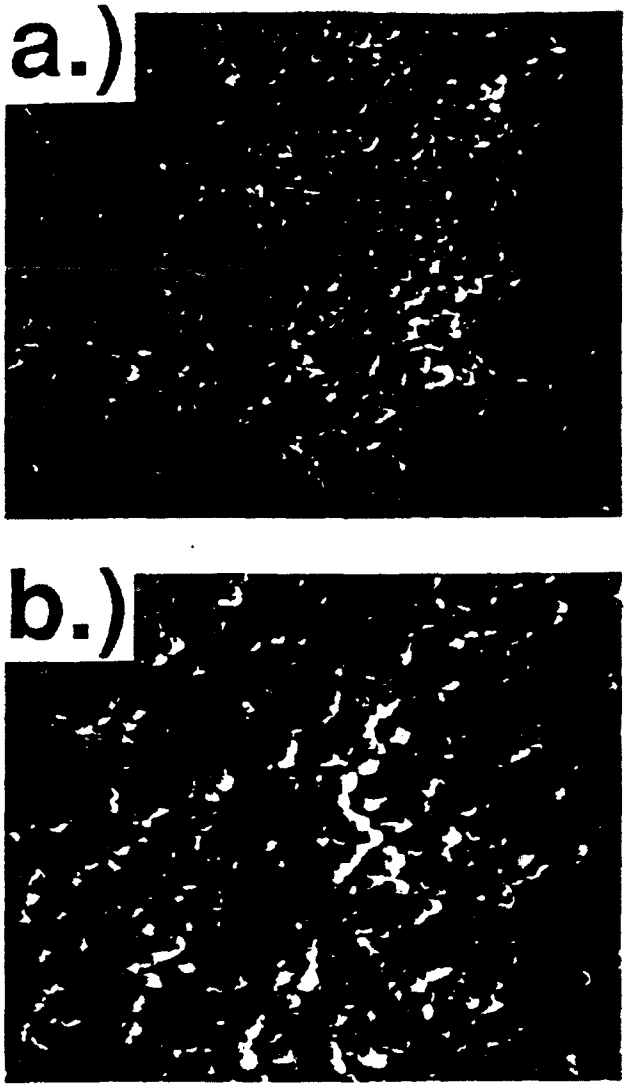

Figure 4

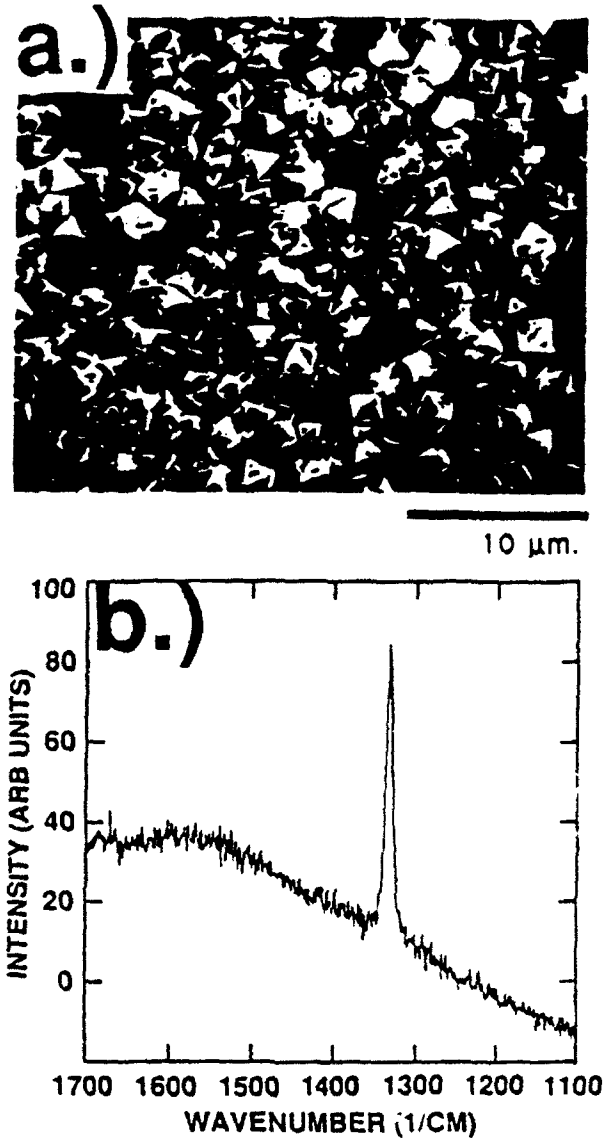
a.)
10 µm.
b.)
INTENSITY (ARB UNITS)
100
80
60
40
20
0
1700 1600 1500 1400 1300 1200 1100
WAVENUMBER (1/CM)

Figure 5

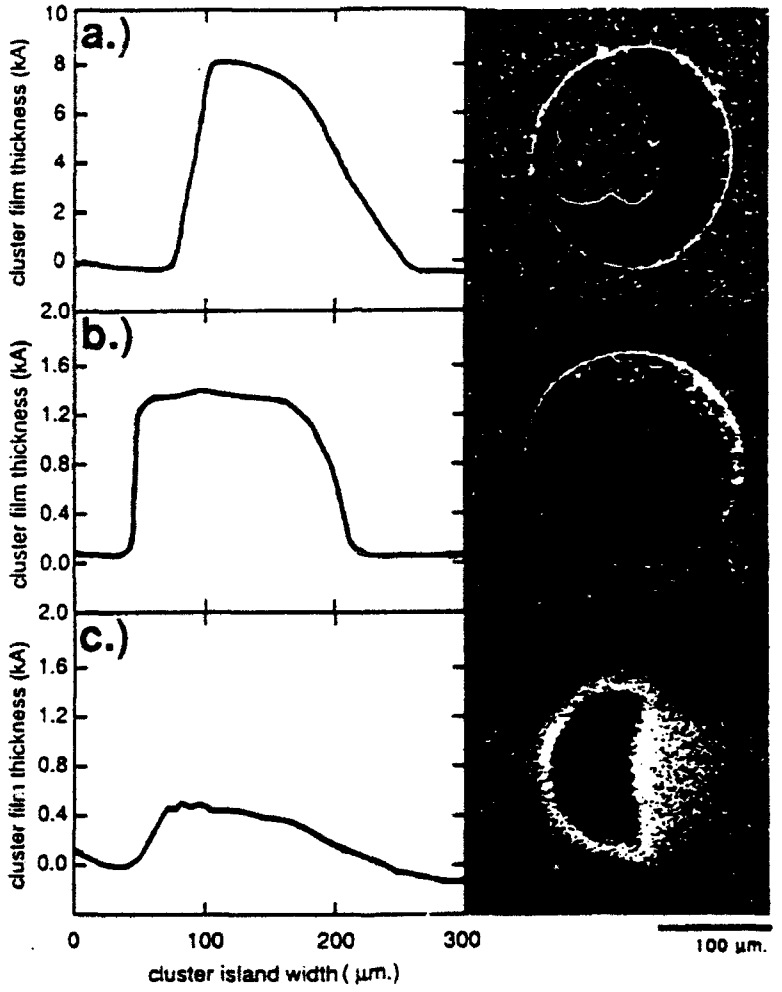
a.)
b.)
c.)
cluster film thickness (kA)
10
8
6
4
2
0
2.0
1.6
1.2
0.8
0.4
0.0
0
100
200
300
cluster island width (µm.)
100 µm.

Figure 6

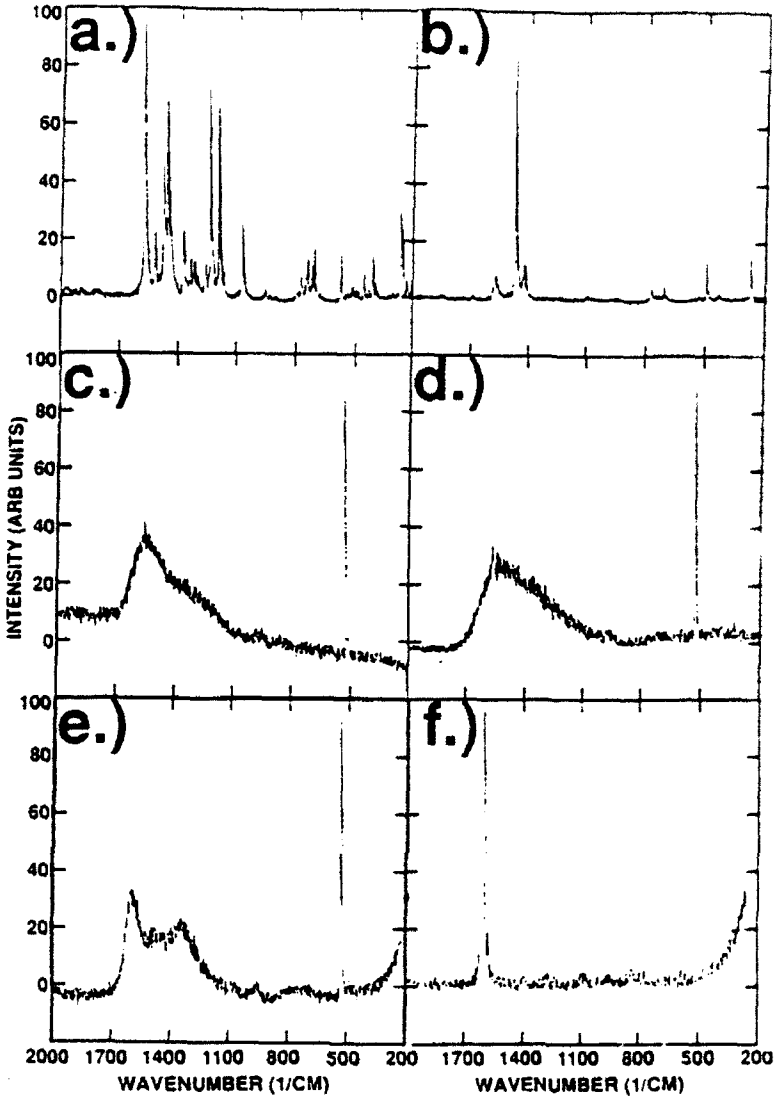

Figure 7

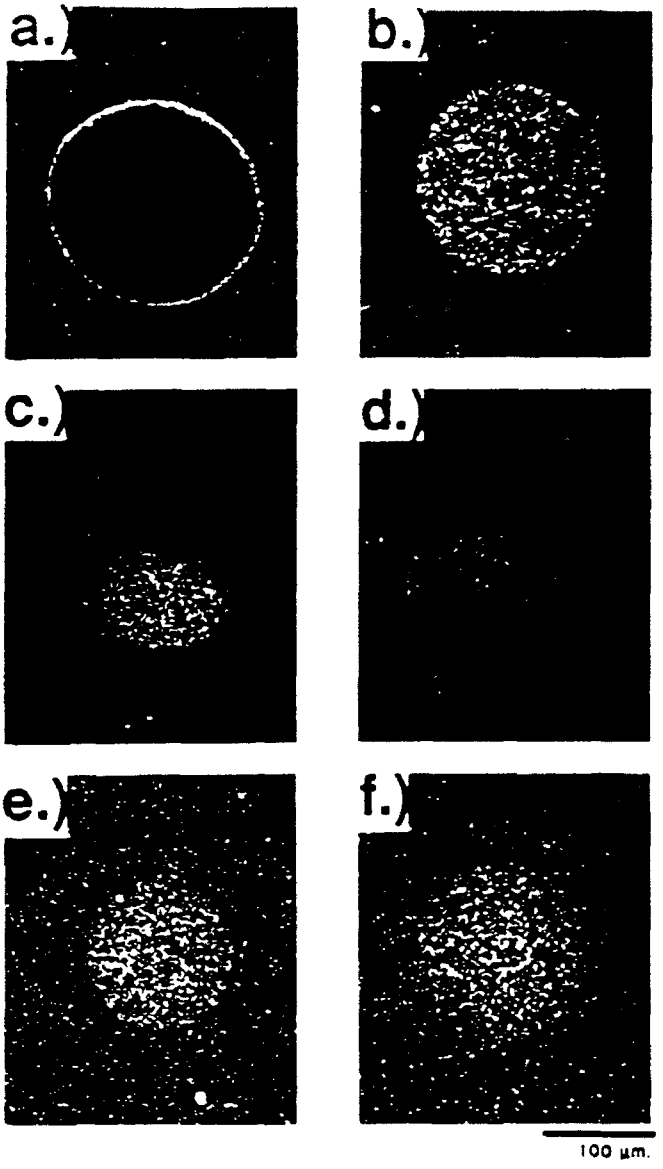

Figure 3

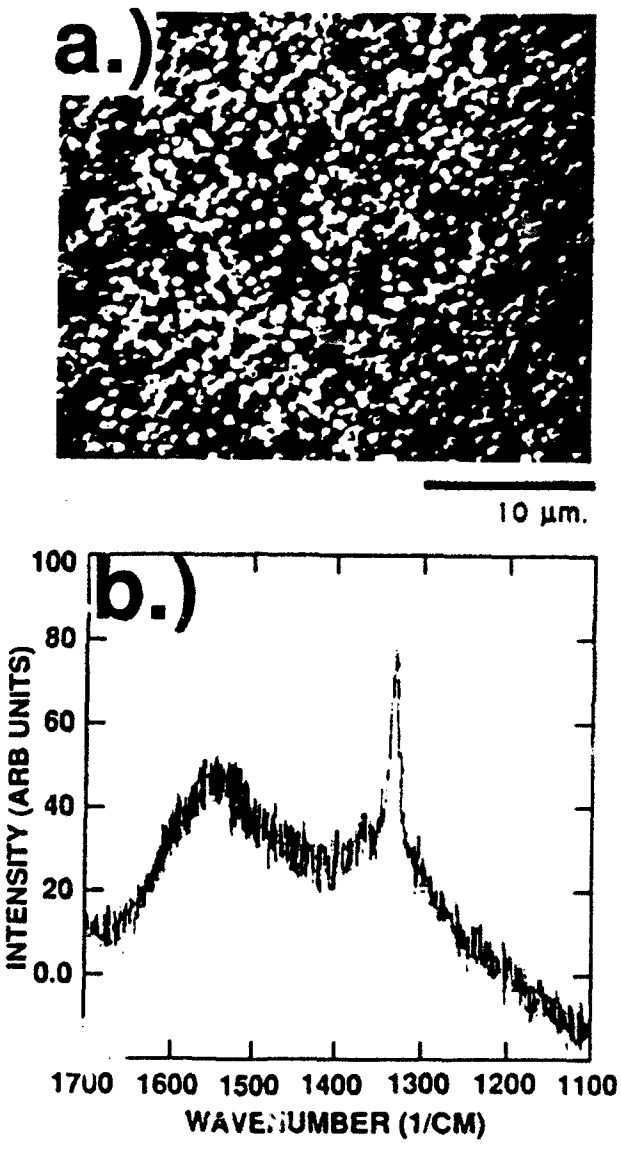
a.)
10 µm.
b.)
100
80
60
40
20
0.0
INTENSITY (ARB UNITS)
1700 1600 1500 1400 1300 1200 1100
WAVENUMBER (1/CM)

Figure 9

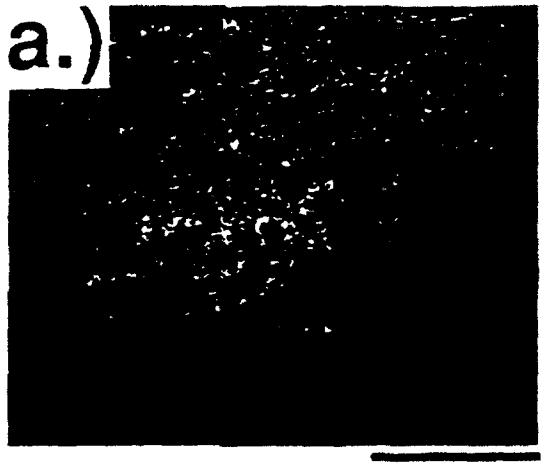

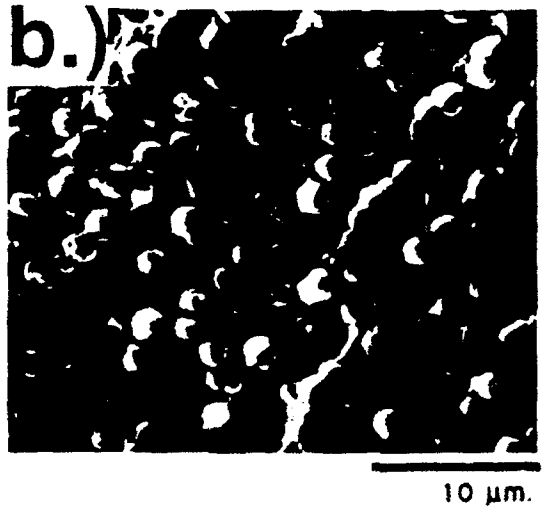

Figure 10

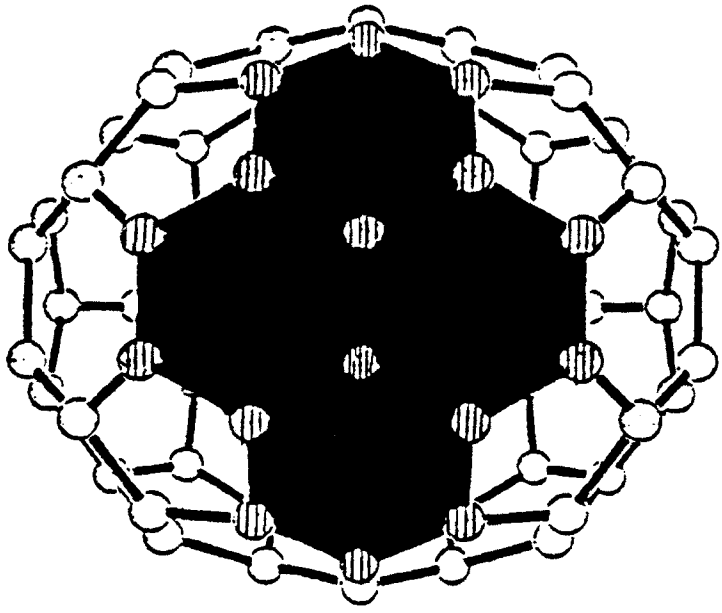

Figure 11

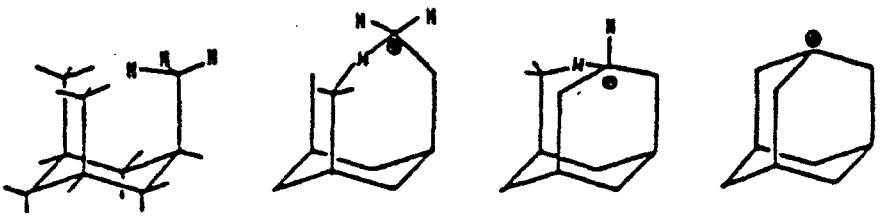

Figure 12

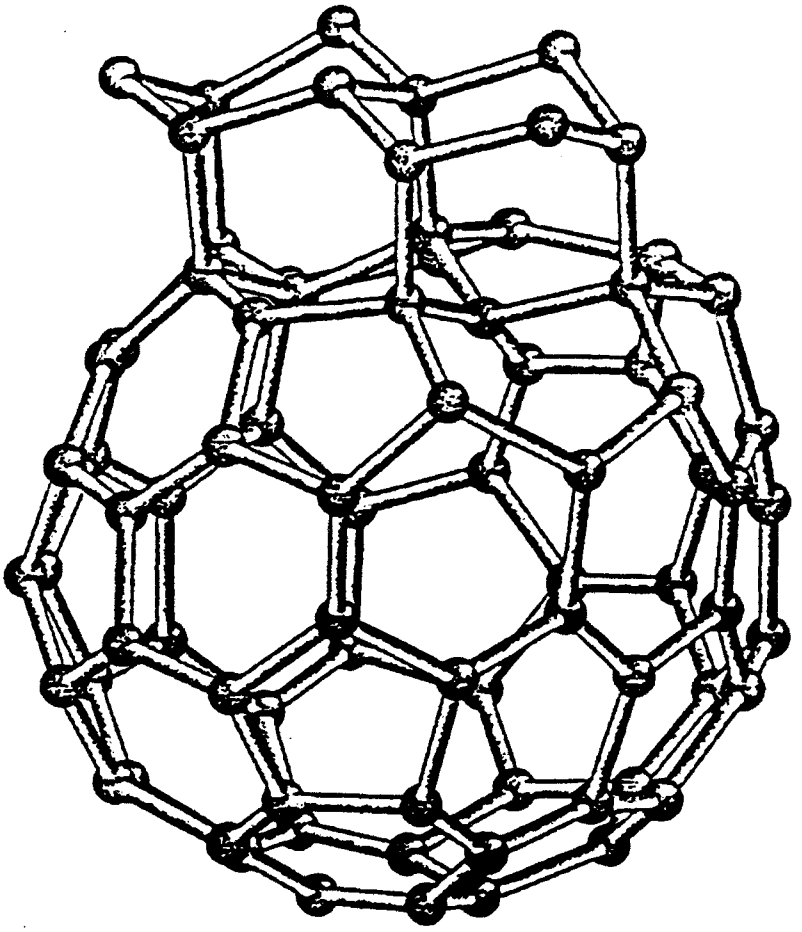

Figure 13

a.)

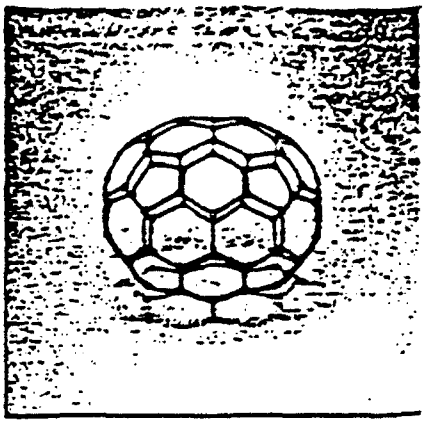

b.)

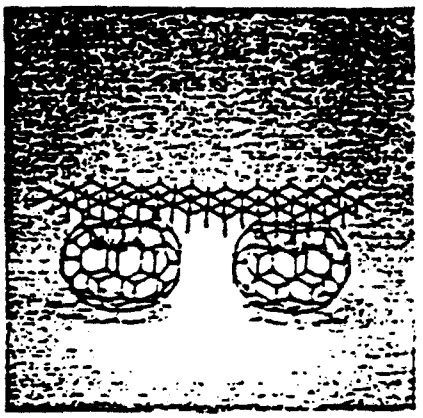

c.)

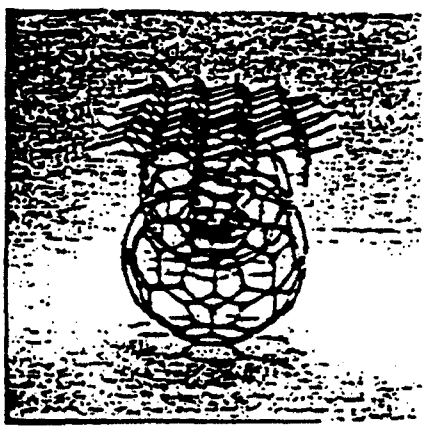

Figure 14

TECHNICAL REPORT DISTRIBUTION LIST - GENERAL

Office of Naval Research (2)*
Chemistry Division, Code 1113
800 North Quincy Street
Arlington, Virginia 22217-5000

Dr. James S. Murday (1)
Chemistry Division, Code 6100
Naval Research Laboratory
Washington, D.C. 20375-5000

Dr. Robert Green, Director (1)
Chemistry Division, Code 385
Naval Air Weapons Center
Weapons Division
China Lake, CA 93555-6001

Dr. Elek Lindner (1)
Naval Command, Control and Ocean
Surveillance Center
RDT&E Division
San Diego, CA 92152-5000

Dr. Bernard E. Douda (1)
Crane Division
Naval Surface Warfare Center
Crane, Indiana 47522-5000

Dr. Richard W. Drisko (1)
Naval Civil Engineering
Laboratory
Code L52
Port Hueneme, CA 93043

Dr. Harold H. Singerman (1)
Naval Surface Warfare Center
Carderock Division Detachment
Annapolis, MD 21402-1198

Dr. Eugene C. Fischer (1)
Code 2840
Naval Surface Warfare Center
Carderock Division Detachment
Annapolis, MD 21402-1198

Defense Technical Information
Center (2)
Building 5, Cameron Station
Alexandria, VA 22314

* Number of copies to forward